Two-dimensional numerical analysis of a thermally generated mesoscale wind system observed in the Mackenzie Basin, New Zealand

Peyman Zawar-Reza and Andrew P. Sturman
Department of Geography, University of Canterbury, New Zealand

(Manuscript received November 2004; revised January 2006)

A mesoscale numerical model was used to perform two-dimensional numerical simulations of a thermally driven circulation, known as the Canterbury Plains Breeze, to examine the effect of key physical mechanisms that determine the intensity of this circulation. The mesoscale model has a 2.5 order turbulence closure scheme with a terrain following coordinate system, and has been previously used successfully for numerical studies in mountainous landscapes. The numerical results confirm observational data showing that during settled weather, the Canterbury Plains Breeze is a significant climatological feature of surface airflow in the Mackenzie Basin in the South Island of New Zealand. This circulation is generated because the elevated plateau creates a horizontal temperature gradient between the air inside and outside the basin at the same height. Other forcing factors, such as the gradient in soil moisture and the land-sea discontinuity, only enhance the intensity of this mesoscale flow by modifying the horizontal temperature gradient.

Introduction

In the past four decades, the importance of local air circulations for air pollution transport, weather forecasting, and land-use management has been realised. Thermally driven circulations, such as sea-breezes and diurnal orographically induced winds, result from interplay between topographic and thermal forcings. Over simple flat terrain, these wind systems can be forecast with a high degree of skill since the underlying physical mechanisms that drive them are well understood, and adequately formulated in atmospheric models. An extensive set of earlier literature reviews is provided by Defant (1951) and Flohn (1969), while books by Oke (1992), Atkinson (1981), Barry (1992) and Whiteman (2000) provide suitable in-depth description of these wind systems.

In New Zealand, observational studies of thermally driven circulations have been reported by McGowan et al. (1995), McGowan and Sturman (1996) and Kossmann et al. (2002). Kossmann et al. (2002) provided a comprehensive analysis of the thermodynamics of local wind systems in the Lake Tekapo region situated in the Mackenzie Basin of the South Island. Numerical analysis of these circulations, using the Regional Atmospheric Modelling System (RAMS; Pielke et al. 1992), has also been described by Zawar-Reza (2000) and Zawar-Reza et al. (2004).

Corresponding author address: Peyman Zawar-Reza, Department of Geography, University of Canterbury, Private Bag 4800, Christchurch, New Zealand
Email: peyman.zawar-reza@canterbury.ac.nz

During the Lake Tekapo Experiment (LTEX) field campaign (Sturman et al. 2003) a persistent easterly wind system was observed in Mackenzie Basin under settled synoptic conditions. The easterly – from here on referred to as the Canterbury Plains Breeze (CPB) – was usually detected in the early afternoon, was of moderate intensity (6–12 m s^{-1}), and blew throughout the basin overwhelming the locally generated circulations. Although its existence is well known to local inhabitants and its intrusive nature disliked by them, previous meteorological studies in the area paid little attention to it, since it was believed to be the inflow of a sea-breeze circulation originating at the coast and then propagating towards the mountain ranges (Fig.1). A visual clue to the existence of the CPB is the formation of waterfall clouds over mountain saddles on days with quiescent synoptic weather conditions, and it is evident that the CPB is capable of transporting large volumes of air from outside the basin. Recently, degradation of air quality in basins has been a major concern in Japan (Kurita et al. 1990). Even though no significant local sources of air pollution exist in these basins, high concentrations of air pollutants are often recorded at night. A wind system (analogous to the CPB that flows into the Mackenzie Basin) is presumed to be an important factor in transporting polluted air from large industrialised plains outside the Japanese basins (Kimura and Kuwagata 1993). Hence, these circulations have the potential to transport air pollutants across large distances and degrade air quality in pristine mountainous areas. Knowledge of such a persistent wind system can also aid in flight safety for local aircraft operators, forecasting early morning clouds (often the CPB transports moist coastal air into the basin which, combined with nocturnal cooling of the basin atmosphere, leads to the formation of basin-wide low stratus cloud in the morning) and soil erosion.

In this paper, RAMS is used in a two-dimensional configuration to determine the mechanism(s) responsible for the forcing of the CPB. Two-dimensional calculations have been used extensively by the scientific community to study thermally and dynamically forced circulations. Several investigators have used the two-dimensional framework to investigate thermally induced flows in complex terrain at a variety of scales. Mannouji (1982) used a hydrostatic, anelastic equation system to study the characteristic features of mountain and valley winds. He concluded that two wind systems are produced by thermal forcings in complex terrain. A slope wind system is produced by the gradient in the local topography, and a larger scale plain-plateau wind produced by regional-scale horizontal gradients in temperature. The latter is also the result of a topographic gradient, except at a much larger scale. His findings were corroborated by Bossert and Cotton (1994), who used the two-dimensional configuration of RAMS to study regional-scale flows over the Colorado mountain barrier. In particular, they supported the scale separation conclusion reached by Mannouji (1982). Kimura and Kuwagata (1993) and De Wekker et al. (1998) also performed numerical simulations to study plain-to-basin winds. An important conclusion reached by De Wekker et al. (1998) is the need for a horizontal temperature gradient to exist at the mountain height for development of plain-to-basin wind systems. Their findings are also in agreement with Mannouji (1982).

Fig. 1 Map of the South Island of New Zealand showing the transect through the Mackenzie Basin.

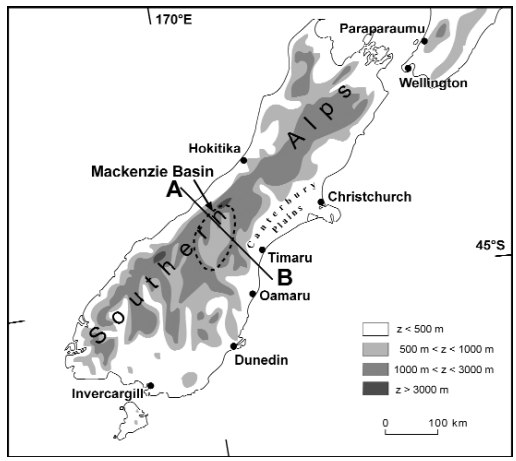

In the following sections, results from twelve two-dimensional numerical simulations are presented. The approach used is to build three simplified topography models in a two-dimensional configuration, roughly representing an east-west cross-section of the South Island through Mackenzie Basin (Fig. 1), and analyse the thermally driven flow that is generated. This way, several forcing mechanisms are investigated for their ability to promote and influence the mesoscale coast-to-basin flow at this locality. The physical forcings investigated are due to spatial variations in:

a) landscape (land-sea contrast), resulting in sea-breeze circulations outside the basin; and
b) variation in rainfall (and hence soil moisture), resulting in inhomogeneous boundary layer development between the plains and the basin.

Numerical modelling

The Regional Atmospheric Modelling System (RAMS) was developed at the Colorado State University, where it was created as a result of merging three different numerical codes (Pielke et al. 1992). The code in its current form is capable of simulating a variety of atmospheric flows. It has been used to study flows at several scales, ranging from flow over buildings to hemispheric circulations. The model contains a full set of subgrid, microphysical, radiative, convective and surface-layer parametrisations. Prognostic models for soil and vegetation temperature and moisture are also included. The model's other capability is a telescoping two-way interactive grid nesting, so that it is possible for a single simulation to represent forcings from a multitude of scales.

A brief description of the three-dimensional equations employed in RAMS is given here; these are basically the Reynold's-averaged Navier-Stokes equations. The horizontal equations of motion (Eqns 1 and 2) are shown below; where term I represents wind acceleration, term II represents advection, term III represents the pressure gradient force, term IV represents Coriolis force, and term V represents turbulent diffusion (for an in-depth discussion on derivation of these equations refer to Pielke 2002):

$$\frac{\partial u}{\partial t} = -u\frac{\partial u}{\partial x} - v\frac{\partial u}{\partial y} - w\frac{\partial u}{\partial z} - \theta\frac{\partial \pi'}{\partial x} + fv + \frac{\partial(u'u')}{\partial x} + \frac{\partial(u'v')}{\partial y} + \frac{\partial(u'w')}{\partial z} \quad ...1$$

$$\frac{\partial v}{\partial t} = -u\frac{\partial v}{\partial x} - v\frac{\partial v}{\partial y} - w\frac{\partial v}{\partial z} - \theta\frac{\partial \pi'}{\partial x} + fu + \frac{\partial(v'u')}{\partial x} + \frac{\partial(v'v')}{\partial y} + \frac{\partial(v'w')}{\partial z} \quad ...2$$

I II III IV V

Horizontal velocity components are represented by u and v; w is the vertical component. π' is the perturbation Exner function, which arises in these equations as a result of replacing pressure with the total Exner function (π) (in mesoscale models, the pressure gradient term is expressed using the Exner function). Total Exner function is defined as:

$$\pi = C_p \frac{T_v}{\theta} \quad ...3$$

where C_p is specific heat of air at constant pressure, T_v is virtual temperature, and θ is the potential temperature. The vertical momentum equation for the non-hydrostatic case is:

$$\frac{\partial w}{\partial t} = -u\frac{\partial w}{\partial x} - v\frac{\partial w}{\partial y} - w\frac{\partial w}{\partial z} - \theta\frac{\partial \pi'}{\partial z} - \frac{g\theta_v'}{\theta_0} + \frac{\partial(w'u')}{\partial x} + \frac{\partial(w'v')}{\partial y} + \frac{\partial(w'w')}{\partial z} \quad ...4$$

I II III IV V

where term IV now represents buoyancy force.

The thermodynamic state of the atmosphere is predicted by Eqn 5; where term I is total heating rate, term II represents horizontal advection, term III represents turbulent flux divergence, and term IV represents radiative flux divergence:

$$\frac{\partial \theta_u}{\partial t} = -u\frac{\partial \theta_u}{\partial x} - v\frac{\partial \theta_u}{\partial y} - w\frac{\partial \theta_u}{\partial z} + \frac{\partial(u'\theta_u')}{\partial x} + \frac{\partial(v'\theta_u')}{\partial y} + \frac{\partial(w'\theta_u')}{\partial z} + \left(\frac{\partial \theta_u}{\partial t}\right)_{rad} \quad ...5$$

I II III IV

θ_u is the ice-liquid water potential temperature. Ice-liquid water potential temperature instead of potential temperature is used in RAMS to avoid specification of latent heat tendencies in Eqn 5. According to Tripoli and Cotton (1981), θ_u remains unchanged in the presence of all water phase changes.

In the non-hydrostatic framework, the equation for mass continuity is expressed as:

$$\frac{\partial \pi'}{\partial t} = -\frac{R\pi_0}{C_v \rho_0 \theta_0}\left(\frac{\partial \rho_0 \theta_0 u}{\partial x} + \frac{\partial \rho_0 \theta_0 v}{\partial y} + \frac{\partial \rho_0 \theta_0 w}{\partial z}\right) \quad ...6$$

Where ρ is air density, C_v is specific heat for air at constant volume, R is the gas constant, and π_0, ρ_0, and θ_0 are synoptic-scale reference values of these variables (Pielke 2002).

In a two-dimensional model framework, variations in one of the horizontal directions (most commonly the north-south) are ignored. Therefore in Eqns 1 to 6, all the terms that include $(\partial/\partial y)$ are identically equal to zero, thereby reducing the number of terms that have to be calculated, resulting in considerable reduction in computation time. Two-dimensional models have been used extensively by the scientific community to study thermally and dynamically forced circulations, even though their results cannot be directly compared with observations. Yet, they provide a valuable tool for gaining insight into flows in complex terrain by stripping away complexities arising from the three-dimensional aspect of nature. The version of RAMS used for this work is designated as 3a. This particular code has been extensively tested by scientists at the Pacific Northwest National Laboratories in Richland, Washington State to study mesoscale circulations, especially in a two-dimensional framework (De Wekker et al. 1998; Whiteman et al. 2000), but also in three dimensions (Fast et al. 1996; Zhong et al. 1996; Doran and Zhong 2000).

Calculation of fluxes of heat, moisture and momentum in the surface layer are based on the Monin-Obukhov similarity theory (Monin and Obukhov 1954), for a horizontally homogeneous flat terrain, under clear-sky conditions. Little is known about the validity of the similarity theory in complex terrain. However, it seems that the similarity theory may be applied in complicated conditions since

numerical models have had relative success under such conditions. RAMS employs a scheme developed by Louis (1979) to estimate the surface layer fluxes via pre-computed approximations of the flux profile functions of Businger et al. (1971). Subgrid vertical eddy mixing coefficients are calculated according to Mellor and Yamada (1974, 1982) with a so-called level 2.5 turbulent kinetic energy (TKE) scheme, including modification for the case of growing turbulence (Helfand and Labraga 1988). A local deformation scheme based on Smagorinsky (1963) is used to calculate horizontal diffusion

Table 1 provides a summary of the twelve simulations conducted for the Mackenzie Basin cross-section. A description of the topographic configurations is provided in the next section. There are three topographic configurations and four different sets of surface characteristics/forcings. For all three sets of topographic simulations, the effect of the land-water contrast generating a sea-breeze and the effect of having dryer soil on the elevated plateau (basin) are tested. From hereon, PLT, MTN and BAS designated simulations are referred to as dry runs and the rest of the simulations are referred to as wet runs.

Two-dimensional simulation development

Topographic configurations

The three topographic configurations used are illustrated in Fig. 2. The simulations designated as PLT are the simplest representation of topography for an east-west cross-section of the South Island (Fig. 2(a)). The plateau and the sloping terrain (~1.1° gradient) in the east of the domain represent Mackenzie Basin and the Canterbury Plains respectively. The 'plateau' topography is symmetric; the elevated surface is 95 km wide and has a constant elevation of 760 m ASL. The 'mountain' runs (MTN) add a degree of complexity to the topography by the addition of a 2000 m high mountain (Fig. 2(b)) to the west of the plateau, a rough representation of the main divide (backbone of the Southern Alps). Consequently, the length of the plateau has decreased to 44 km, which is approximately the diameter of Mackenzie Basin. The mountain has a half-width of 40 km and an average slope of ~4°. Finally, the basin characteristics are introduced to the topographic configuration by the addition of a 1200 m mountain to the east of the plateau representing an approximation of the Two Thumb Range (Fig. 2(c)).

Four scenarios are tested for each of the topographic configurations (Table 1):

(a) The PLT, MTN and BAS designated simulations (dry runs) have a soil moisture content of 15 per cent specified for the whole land surface (this value represents the percentage of total water capacity which the soil holds). The objective of these simulations is to study the effect of topography on the mesoscale circulation without the added complexity introduced by variations in boundary-layer development associated with different land-surface characteristics.

(b) The PLTO, MTNO and BASO designated simulations are initialised with the same soil moisture content as in 1), except ocean-surface characteristics are added to the outer domain to represent the ocean around the South Island (Fig. 2). The sea-surface temperature is specified at 16°C, and the coast is placed at 40 km from the plateau (approximately the distance between Mackenzie Basin and the east coast of the South Island). The objective here is to investigate how the ocean around the South Island affects the development of the CPB.

Table 1. Summary of the two-dimensional RAMS experiments.

Name	*Description*	*Purpose*
PLT	Symmetric plateau	To examine response to surface heating alone
MTN	Mountain and plateau	
BAS	Basin topography	
PLTO	Surrounded by ocean	To examine the influence of the ocean
MTNO		
BASO		
PLT-M	Higher soil moisture on the plains	To examine the effect of variable ground wetness
MTN-M		
BAS-M		
PLTO-M	Higher soil moisture on the plains	To examine the combined effect of the above two influ-
MTNO-M	and surrounded by ocean	ences
BASO-M		

Fig. 2 **Topographic configurations used to represent the Mackenzie Basin cross-section: (a) a simple plateau (PLT); (b) mountain plus plateau (MTN); (c) basin between main divide and foothills (BAS). The horizontal lines and arrowheads indicate where wet soil was placed in the wet runs. The U-component of wind velocity shown in Fig. 15 was extracted from the position indicated with u and a vertical arrow over the elevated plateau. East (west) is to the right (left) side of the cross-sections.**

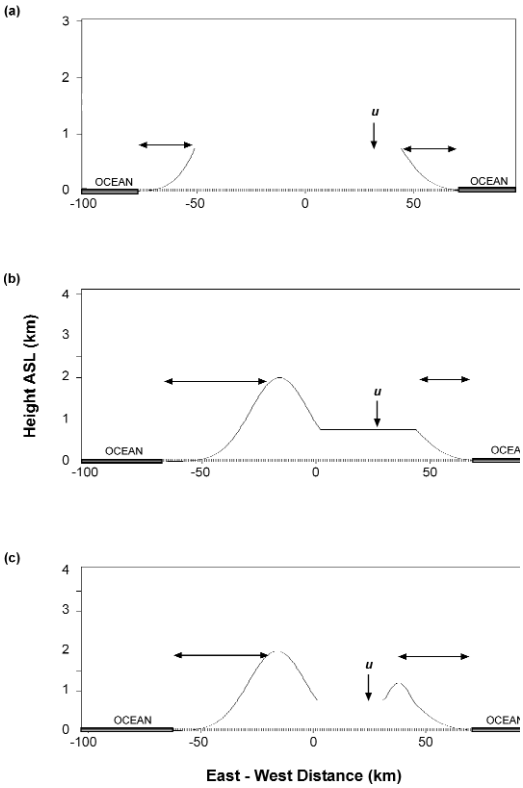

(c) The PLT-M, MTN-M and BAS-M designated simulations have no ocean characteristics, but the soil moisture content has been increased to 35 per cent outside the plateau (Fig. 2). The purpose of these simulations is to isolate the effect of regional-scale variations in precipitation, and hence soil moisture, on the thermally induced circulation system. The climate of Mackenzie Basin is typical of inner montane basins of the South Island where the rain-shadow effects of the surrounding ridges result in annual precipitation rates of only 600 mm. Therefore the soil moisture content in the basin is usually lower than the surrounding plains.

(d) The runs designated as PLTO-M, MTNO-M and BASO-M examine the combined effects of the presence of the ocean and the variability in soil moisture on the mesoscale circulation.

The whole domain uses the desert parametrisation as a surface characteristic (which does not take into account influences from vegetation). Results of tests (not shown here) indicate that the main features of the CBP are not affected by using different land-surface characteristics (i.e. grass or irrigated crop) outside the elevated plateau.

Model setup

A summary of the model setup is given in Table 2. Grid nesting was not employed for these runs. A grid spacing of 1 km was chosen for the horizontal direction, and the vertical grid spacing starts at 35 m at the surface increasing with a ratio of 1.12 to 1000 m near the model top, which is situated at 19 km above sea level. Therefore, the lowest model computational level is at about 25 m above ground level, so that with this vertical resolution, 10 grid-points are located within 500 m from the ground. The upper boundary is a rigid lid, and the eastern and western lateral boundaries employ the radiative condition following Klemp and Wilhelmson (1978a, 1978b), and the northern and southern lateral boundaries use the cyclic boundary condition. A damping scheme is applied to the top ten vertical layers where the amplitudes of vertically propagating gravity waves and other disturbances are gradually suppressed to reduce wave reflection from the rigid lid. Application of the damping scheme is necessary when the domain contains topography with significant variation in elevation.

Initialisation

For this set of simulations, the model was initialised at 1900 NZST on 11 February 1999 (0700 UTC, 11 February 1999) and run continuously for a 30-hour period. The integration started with the atmosphere at rest (initial wind field was set to zero), so that the resulting wind field is a response to terrain cooling and heating alone. The initial vertical profiles of temperature and humidity were measured by an instrumented aircraft as described by Kossmann et al. (2002). The initial soil temperature was set to 20°C for all 11 soil levels, with the deepest layer situated at 0.5 m.

Simulation results

Plateau simulations

Turbulent transfer of sensible heat from the surface caused the boundary layer to grow to a depth of

Table 2. Summary of model setup.

Number of east-west nodes	465
Number of north-south nodes	5
Number of vertical nodes	42
Dx, Dy (m)	1000
Dz (m)	35m at bottom, 1000m at top
Vertical stretch ratio	1.12
Model top (km)	19
Dt (s)	10
Soil type	Sandy loam
Vegetation type	Desert (no vegetation)
Soil moisture percentage of dry soil	15
Soil moisture percentage of wet soil	35
Coriolis force	Activated
Time differencing	Leapfrog
Radiation scheme	Long wave and short wave (Chen and Cotton 1983)

approximately 700 m throughout the domain by 1200 NZST (Fig. 3(a)). Heating of the slope generated an upslope circulation, with a weak easterly wind (~2 m s^{-1}) over the plateau's edge. A baroclinic zone formed between the air over the plateau and the air at the same elevation over the plain, with a horizontal potential temperature difference of about 2 K. The reason for this thermal contrast is that air over the elevated plateau gets heated much more quickly than air at the same elevation over the plains due to its proximity to the ground. By 1400 NZST, the boundary-layer depth had increased to 1200 m (Fig. 3(b)), the weak easterly had encroached onto the plateau from the eastern slope, and the difference of potential temperature was now about 2.5 K across the baroclinic zone. The easterly continued to propagate westward at 1600 NZST and had penetrated approximately 19 km onto the plateau (Fig. 3(c)). As the boundary-layer depth is higher than the elevation of the plateau, the differential horizontal temperature gradient across the baroclinic zone remained close to 2.5 K. This plateau circulation is similar to that simulated by Bossert and Cotton (1994) over a plateau 3000 m high and is induced by the asymmetry of the topography at the plateau's edge. Mannouji (1982) also described the numerical development of a similar circulation system over his 2000 m high plateau, which he termed a plain-plateau breeze.

The forcing mechanism for the development of the density current in the PLT run is analogous to sea-breeze and along-valley circulations. The relatively warmer air mass over the plateau leads to a hydrostatically lower pressure there, creating a pressure gradient force directed towards it, leading to relatively colder air being drawn from the atmosphere above the plains (cold air advection). The hydrostatic approximation can be written as:

$$\Delta P = g \int_{z_1}^{z_2} (r_{\text{plain}} - r_{\text{plateau}}) \mathrm{d}z \qquad ...7$$

where ΔP is the difference between surface pressure over the plateau and pressure at the same elevation over the plains, z_1 is plateau floor height, z_2 is the height where horizontal temperature gradients diminish, ρ is the air density (over the plains and plateau), and g is the gravitational acceleration. Cold air advection by the plain-to-plateau circulation ultimately results in depressing of the mixed-layer height over the plateau. This depression of mixed-layer height due to cold air advection becomes more pronounced in the subsequent runs. In summary, the primary forcing for the density current generated by the PLT run seems to be the regional-scale differential heating of air due to proximity to the ground.

The addition of the ocean surface to the domain has a significant impact on the development of the density current for the PLTO experiment. At 1400 NZST, there was a difference in boundary-layer development over the plain (Fig. 4(a)) due to a westward-propagating sea-breeze circulation that had been generated. Behind the sea-breeze front, the propagating marine air caused the formation of the coastal mixed layer. The cold air advection and subsidence induced by the return flow resulted in a decrease of the mixed-layer depth towards the coast. This depression of the mixed-layer depth was also noted by Anthes (1978) and Lu and Turco (1994) with their two-dimensional simulations. The boundary-layer temperature structure close to the plateau was not affected by the sea-breeze at this time, so that the CPB still had the same characteristics as the PLT run. It is apparent that the sea-breeze and the CPB are two different circulation systems, generated by different

Fig. 3 **Isopleths of the u-component wind (m s^{-1}) on the right and the potential temperature field (K) on the left for the plateau simulation (PLT) at (a) 1200, (b) 1400 and (c) 1600 NZST. Dashed isopleths indicate negative u-component (winds blowing from right to left). Contour interval is 0.5 K for the potential temperature fields, and 0.3 m s^{-1} for the winds.**

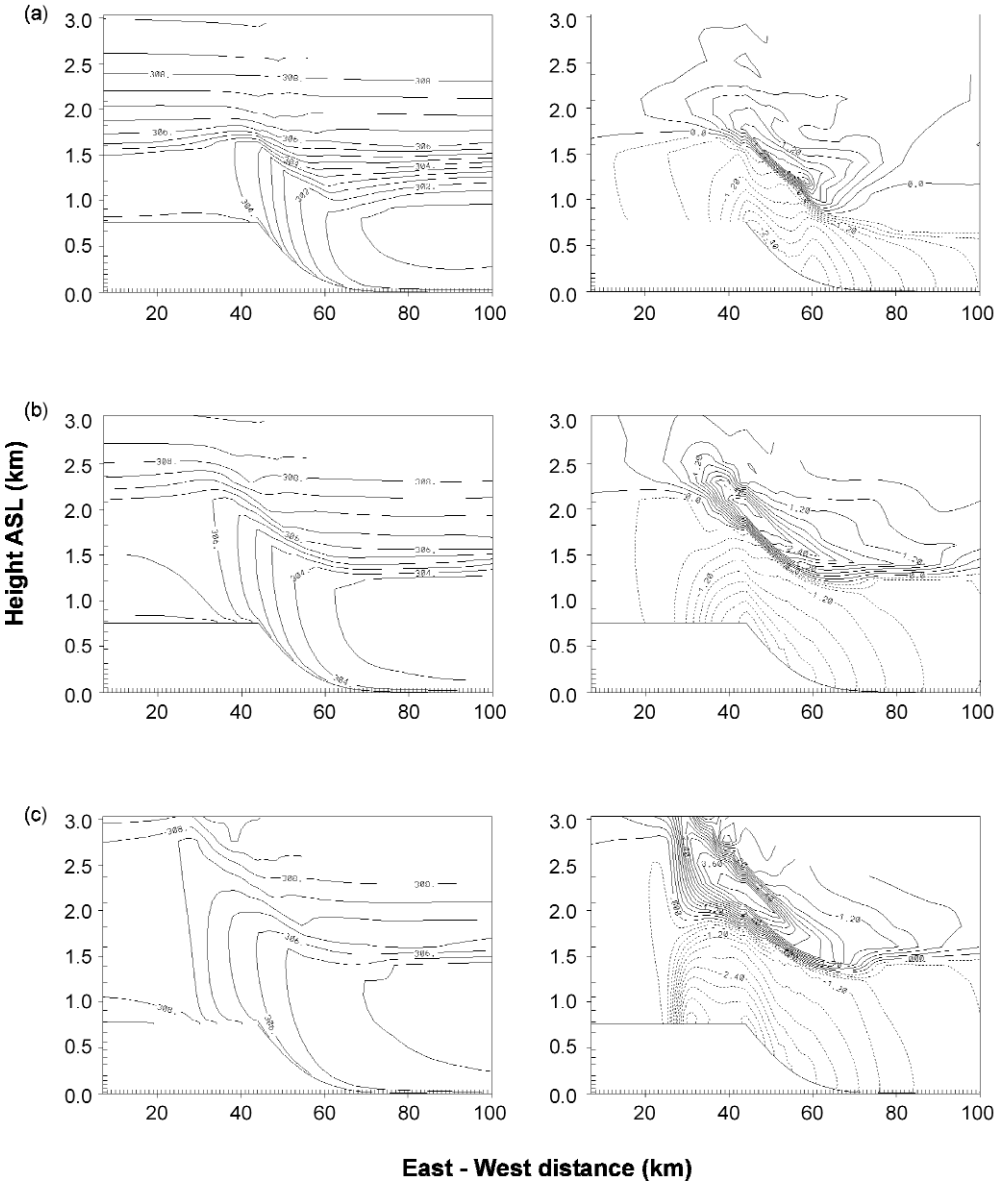

physical forcings. The sea-breeze front was about 18 km from the plateau's edge (propagating westward at a speed of 6.4 m s^{-1}), while at the same time, a plain-to-plateau circulation with a wind speed of about 3.2 m s^{-1} was blowing over the plateau. The front of the current had penetrated 5 km onto the plateau. The mixed-layer depth had increased to 1200 m over the plateau (similar to the PLT run), and the development of the boundary layer over the plains remained restricted due to the cold air advection associated with the sea-breeze. As a result, the horizontal temperature difference across the baroclinic zone was about 4.5 K.

Fig. 4 **Isopleths of the u-component wind (m s^{-1}) on the right and the potential temperature field (K) on the left for the plateau with the ocean simulation (PLTO) at (a) 1400 and (b) 1600 NZST. Dashed isopleths indicate negative u-component (winds blowing from right to left). Contour interval is 0.5 K for the potential temperature fields, and 0.5 m s^{-1} for the winds.**

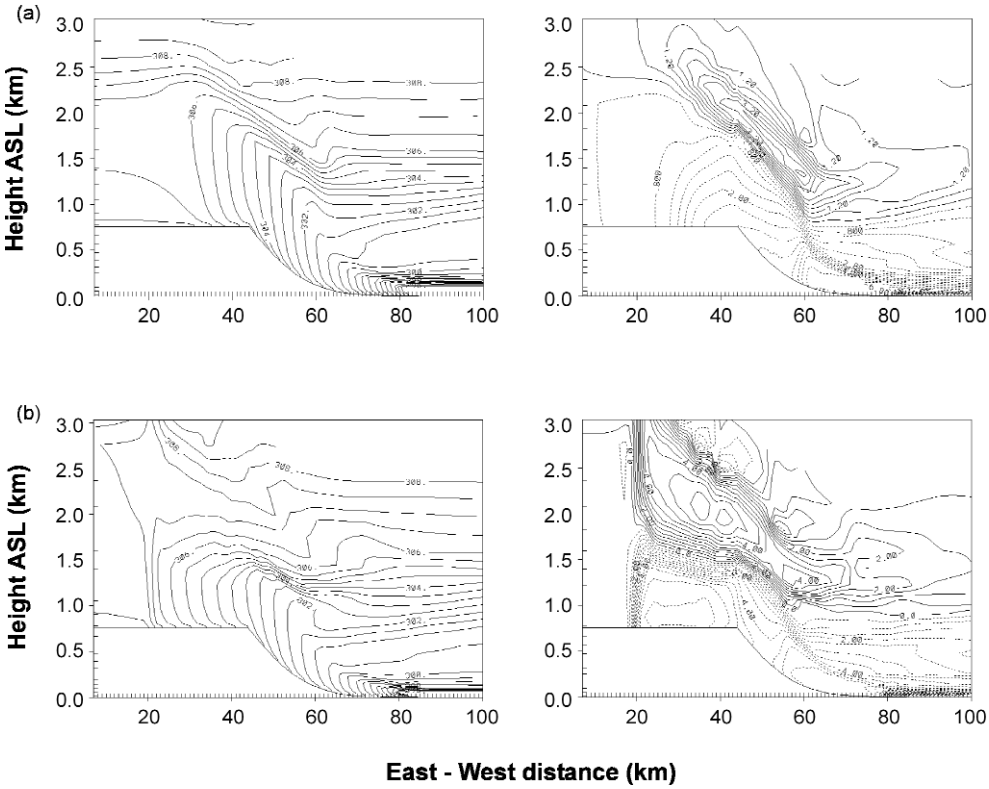

The 1600 NZST (Fig. 4(b)) fields show evidence of a well-developed CPB current with an intensity of 6.0 m s^{-1} over the plateau which had propagated about 26 km to the west, while the horizontal temperature difference had increased to about 5.5 K. This experiment suggests that sea-breeze formation on the coast due to land-sea temperature contrasts has an indirect impact on the CPB over the plateau. By depressing the boundary-layer height over the plains, the sea-breeze increases the horizontal temperature gradient at the regional scale, intensifying the CPB as a result.

Variation in soil moisture content also has a dramatic impact on the development of the CPB (PLT-M simulations). At 1200 NZST (Fig. 5(a)), the mixed layer over the plains had only grown to a depth of 400 m compared with the depth of 800 m over the plateau. Already, a horizontal temperature difference of about 3 K existed across the baroclinic zone. An understanding of soil moisture effects on boundary-layer growth can be gained by examining the surface energy balance equation that controls the turbulent transfer of heat from the surface. This relationship can be written in simple form as:

$$Q^* = Q_E + Q_H + Q_G \qquad ...8$$

where Q^* is the net radiation, Q_H the sensible heat flux, Q_E the latent heat flux, and Q_G the heat flux into/out of the soil (Oke 1992). The sensible (Q_H) and latent (Q_E) heat flux terms can be expanded into:

$$Q_H = \rho C_P \, C_d \, u \, (T_s + T_a) \qquad ...9$$

$$Q_E = \rho L \, C_d \, u \, (q_s + q_a) \qquad ...10$$

Fig. 5 As in Fig. 4 but for the PLT-M simulation at (a) 1200 and (b) 1600 NZST.

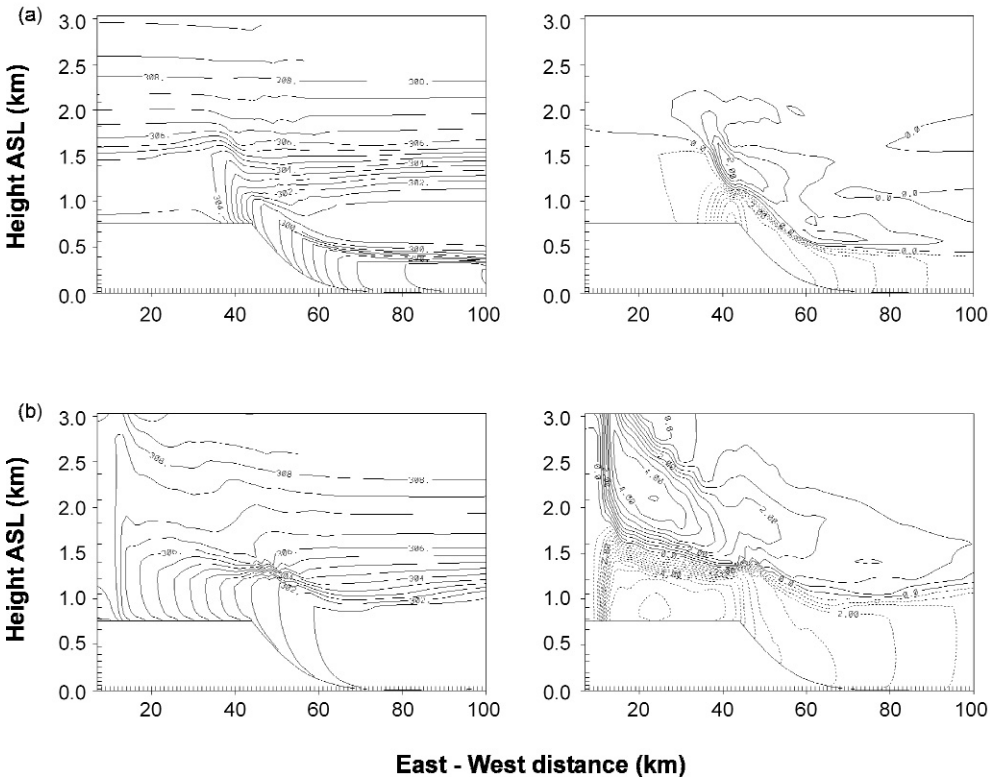

where ρ is the air density, C_P is the heat capacity of air at constant pressure, C_d is the drag coefficient, u is the wind speed close to the surface, T_s is surface temperature, T_a is air temperature close to the surface, L is the latent heat of vaporisation, q_s is the surface mixing ratio, and q_a is the mixing ratio of air close to the surface. When the soil contains more moisture, q_s will be greatly increased leading to partitioning of more of the net radiation into latent heat. The reduction of sensible heat flux results in a cooler and hence shallower boundary layer over the more moist plains.

Similar to the PLT run, the mixed-layer depth over the plateau had grown to a depth of 1200 m by 1400 NZST (not shown), whereas it had only grown to a depth of about 500 m over the plains. With the increase of the horizontal temperature gradient to about 6 K, the CPB had intensified to 4 m s^{-1}, and penetrated 20 km onto the plateau. At 1600 NZST (Fig. 5(b)), the mixed layer had grown to a height of 1 km over the plains, although it was 4 K colder than the mixed layer simulated by the PLT run. Cold air advection due to CPB depressed mixed-layer development over the plateau, while the easterly wind was blowing with an intensity of 6 m s^{-1}. The airflow penetrated 30 km onto the plateau, which is 5 km further than the PLTO run.

The characteristic features of the CPB are the same for the PLTO-M sets of simulations (Fig. 6; only the 1600 NZST isopleths are shown). Since the higher soil moisture over the plains resulted in a reduced sensible heat flux near the coast, the sea-breeze circulation was not as vigorous as the PLTO run. A very shallow boundary layer was formed over the coastal plain as a result of the combined effect of a reduced sensible heat flux, due to higher soil moisture, and cold air advection by the sea-breeze.

Fig. 6 As in Fig. 4 but for the PLTO-M simulation, at 1600 NZST.

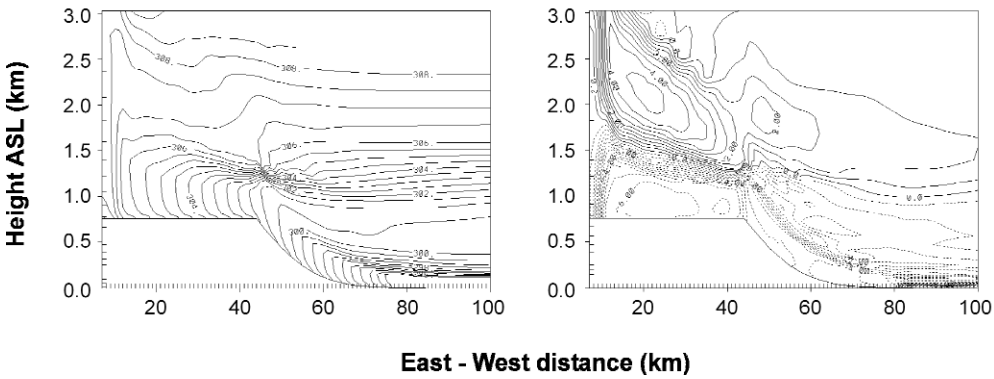

Mountain simulations

In this section, the interaction of the CPB with the plain-to-mountain wind (Whiteman 2000) is investigated. The interaction of mountain flows and sea-breezes were first studied numerically by Mahrer and Pielke (1977). They represent the closest situation to that observed in Mackenzie Basin. Mahrer and Pielke (1977) found that the circulations combined to produce more intense flows during the day. Lu and Turco (1994) found that the coupling of flows is a function of:

(a) the mountain height influencing the sea-breeze;
(b) the distance of the land-sea discontinuity from the mountain;
(c) the vertical temperature profile of the atmosphere.

It is therefore of interest to find out if the Southern Alps have a similar influence on the development of the CPB.

At 1200 NZST, the boundary-layer thermal structure over the plains generated by this run was very similar to that of the PLT simulation (Fig. 7(a)). Heating of the slopes generated a symmetric upslope circulation on both sides of the 2000 m mountain (Fig. 7(a); only the eastern slopes shown). This upslope circulation is similar to the simulation over a 900 m mountain made by Mahrer and Pielke (1977). Due to the horizontal pressure gradient caused by the mountain, a weak easterly flow had already been generated over the plateau (Fig. 7(a)), while an easterly flow was also evident at the plateau's edge, similar to the PLT run. The density current was well developed by 1400 NZST with an intensity of 3.2 m s^{-1}, and had propagated about 20 km onto the plateau (not shown). In this experiment, the plain-to-mountain wind and the CPB circulations are not coupled, suggesting that the forcings that induce each flow are quite distinct. By 1600 NZST (Fig. 7(b)), the whole plateau was dominated by an easterly flow with an intensity of about 3.5 m s^{-1}. Therefore for this dry run, the characteristic features of the CPB circulation were unaffected, except that the flow was intruding into a weak dominant easterly flow set up by the presence of the mountain.

Results for the MTNO, MTN-M and MTNO-M at 1400 NZST are illustrated in Fig. 8. The characteristics of the boundary-layer development over the plains remains the same as the plateau simulations, and the characteristic features of the CPB are also unaffected by the presence of the mountain. This suggests that for the terrain configuration of the two-dimensional simulations, the mountain is so far from the plateau's edge (the source region for the CPB) that it does not significantly interfere with its development. The reduction in mixed-layer growth and thermal structure over the plains due to cold air advection by the sea-breeze, and the high soil moisture content still have the strongest influence on the strength of the CPB.

Basin simulations

Thermally induced flows that transport air into basins have been called plain-to-basin winds. De Wekker et al. (1998) performed a series of two-dimensional simulations with the same version of RAMS used here, to numerically study the characteristics of this particular circulation. Several important differences exist

Fig. 7 **Isopleths of the u-component wind (m s^{-1}) on the right and the potential temperature field (K) on the left for the mountain simulation (MTN) at (a) 1200 and (b) 1600 NZST. Dashed isopleths indicate negative u-component (winds blowing from right to left). Contour interval is 0.5 K for the potential temperature fields, and 0.5 m s^{-1} for the winds.**

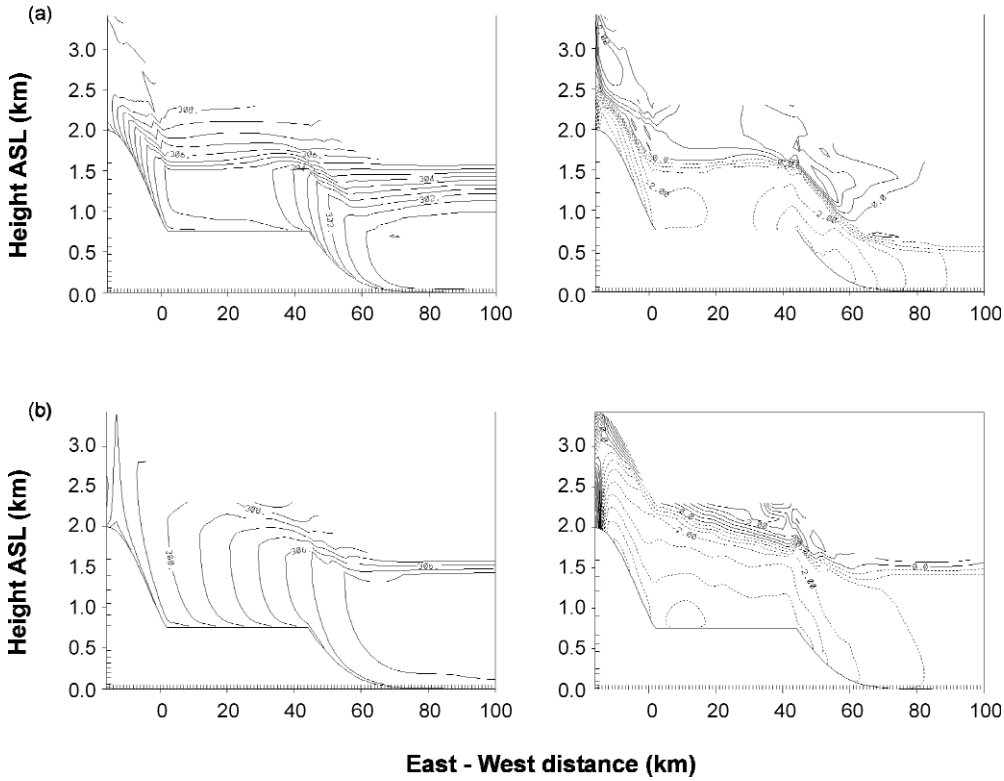

between their simulations and the ones presented in this section. Although they used a variety of topographic configurations, their basins were always symmetrical (both ridges always had the same elevation). They also did not investigate the influences of inhomogeneous soil properties, or the coastal influences on the plain-to-basin circulation. De Wekker et al. (1998) concluded that the plain-to-basin wind:

(a) intrudes into the basin after the cessation of upslope winds on the basin side slope, when the surface sensible heat flux changes sign; and

(b) the intrusion time does not significantly vary in response to changes in basin configuration.

In this study, it was found that in the 'basin' experiment, designated as BAS, the boundary-layer thermal structure developed in the same way as the previous set of dry runs (Fig. 9), although heating of the slopes of the 1200 m mountain on the eastern side of the basin generated upslope winds on both sides of the ridge (Fig. 9(a)). However, because of the horizontal temperature gradient across the ridge, the easterly upslope flow had already begun to overwhelm the westerly flow generated by the shorter western slope by 1200 NZST. As a comparison, since the horizontal thermal structure remained roughly symmetric around the 2000 m ridge, the upslope flows on both sides of the higher ridge converged at the top (see also Fig. 7). By 1400 NZST, the density current had overwhelmed the upslope flow on the basin side and propagated down the slope with a wind speed of 3.2 m s^{-1} (Fig. 9(b)). The intrusion occurred three hours before the surface sensible heat flux changed sign. By 1600 NZST, the plain-to-basin wind exceeded 5 m s^{-1}, particularly over the eastern side of the basin (Fig. 9(c)). Hence, it seems that the asymmetric basin topography (unequal ridge heights) has a significant impact on the intrusion time of the CPB (plain-to-basin wind).

Fig. 8 As in Fig. 7 but for the (a) MTNO, (b) MTN-M and (c) MTNO-M simulations, all at 1400 NZST.

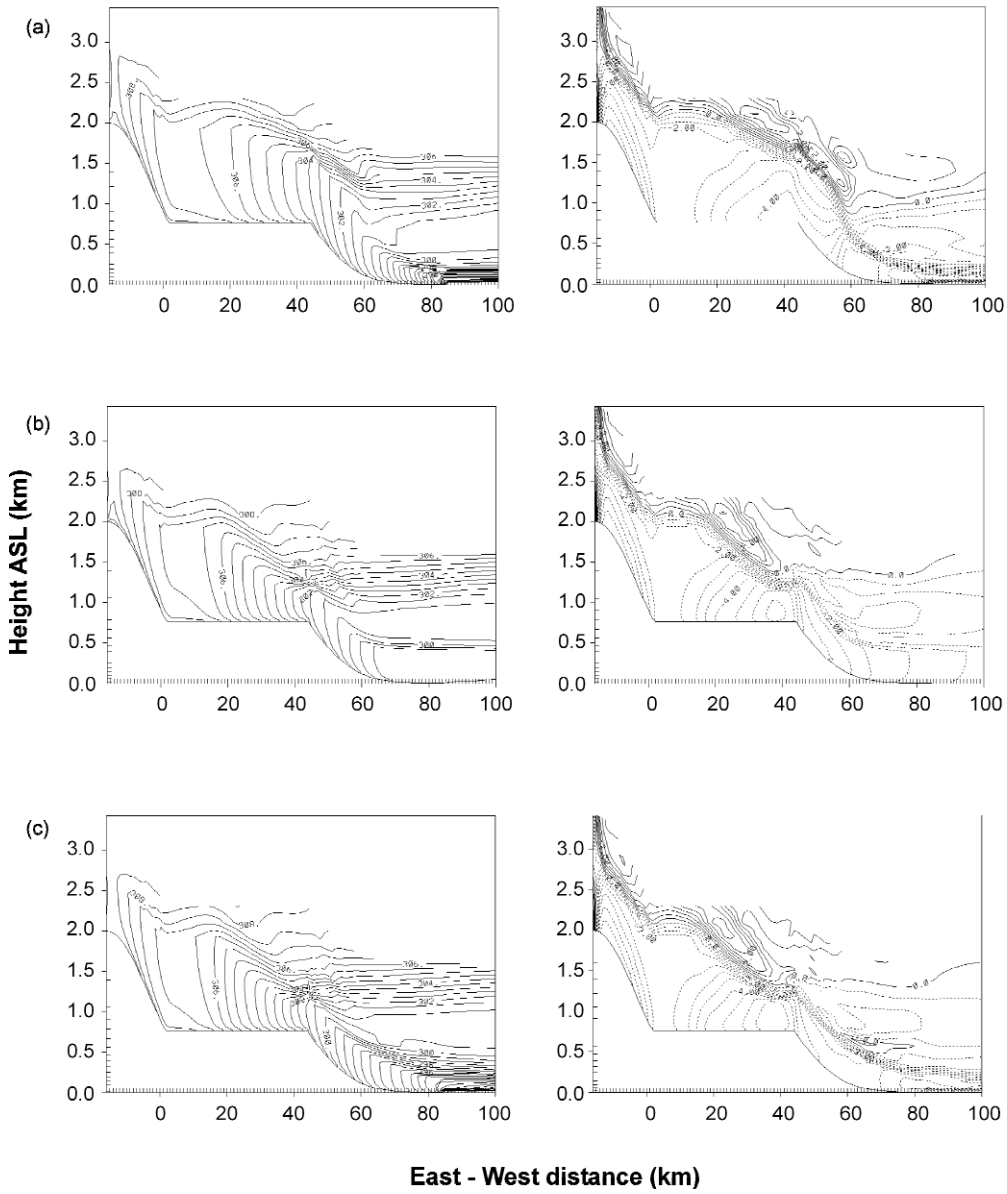

Figure 10(a) shows the results of the introduction of ocean to the domain (BASO) at 1600 NZST. Similar to the basin run, there is a slight intrusion of the density current onto the basin side slope by 1200 NZST (not shown), with an intensity of 2 m s^{-1}. As before, a sea-breeze front is evident over the plains by 1400 NZST (not shown). By 1600 NZST (Fig. 10(a)), the CPB had propagated westward 5 km further than the dry run, since there was a slight increase of 1-2 m s^{-1} in its wind speed.

The results from BAS-M and BASO-M runs at 1600 NZST are shown in Figs 10(b) and 10(c). There is no significant difference between the thermal structures of the boundary layer over the plains above the plateau height between these two simulations. This leads to the development of a similar plain-to-basin circulation sys-

Fig. 9 **Isopleths of the u-component wind (m s^{-1}) on the right and the potential temperature field (K) on the left for the basin simulation (BAS) at (a) 1200, (b) 1400 and (c) 1600 NZST. Dashed isopleths indicate negative u-component (winds blowing from right to left). Contour interval is 0.5 K for the potential temperature fields, and 0.5 m s^{-1} for the winds.**

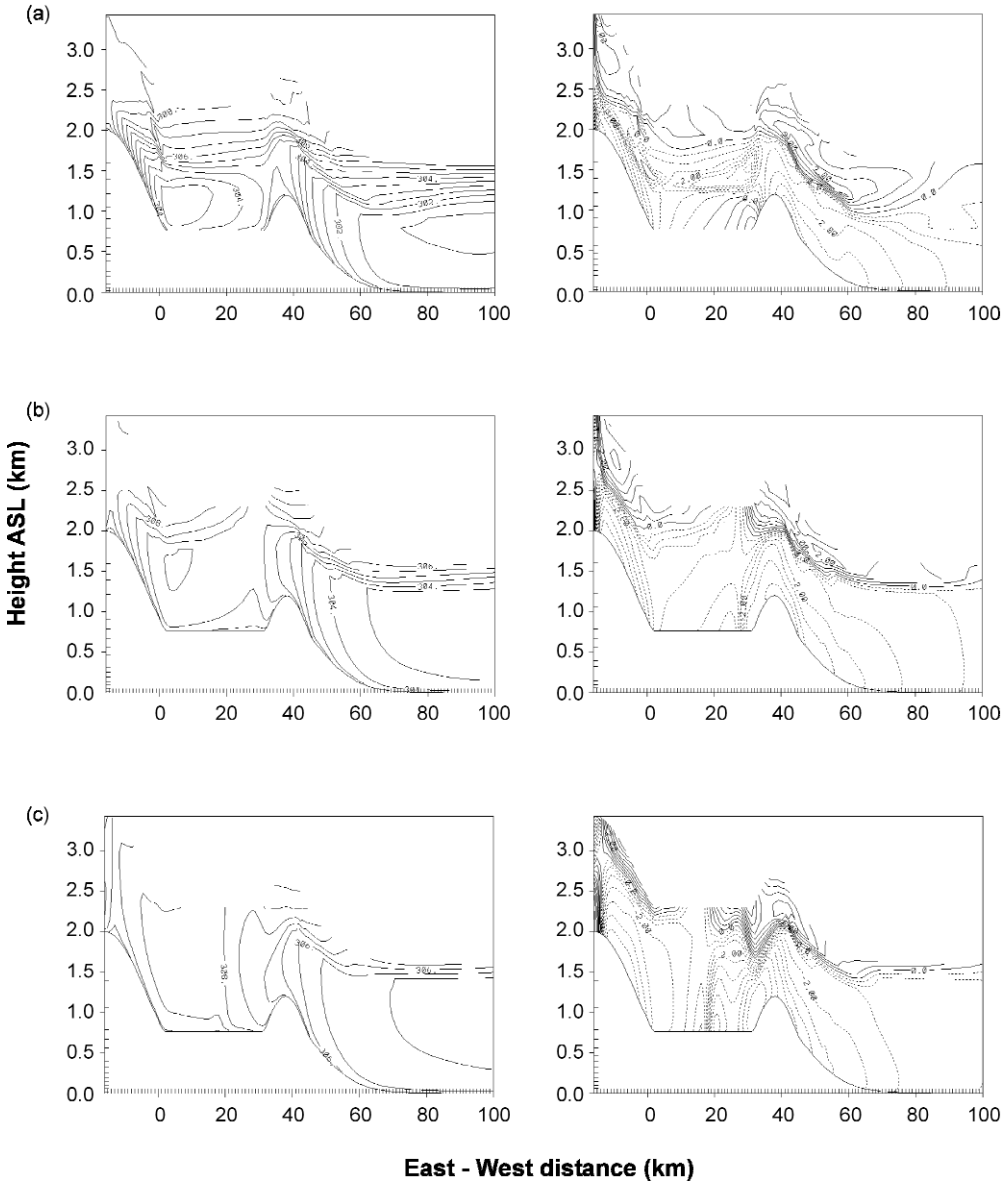

tem in these two runs. As before, the existing inversion layer above plateau height was not eroded because of the prevention of mixed-layer growth due to cold air advection by the sea-breeze and/or decrease in sensible heat flux from the surface due to high moisture content of the soil. The main differences between each of the basin simulations clearly occur over the coastal plains to the east, as shown in Figs 10(a)-(c).

Fig. 10 As in Fig. 9 but for the (a) BASO, (b) BAS-M and (c) BASO-M simulations, all at 1600 NZST.

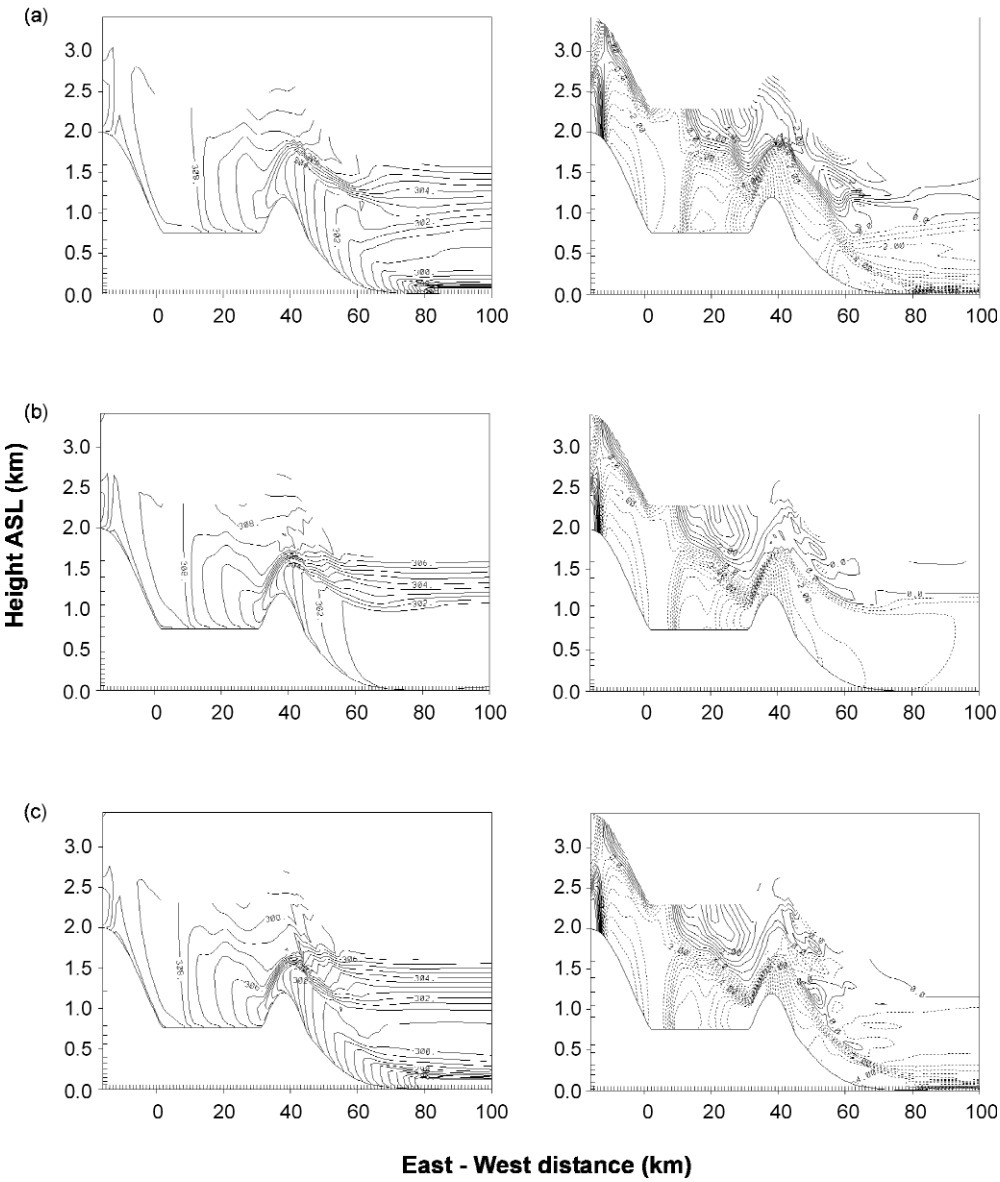

Discussion of results

The numerical simulations show that the CPB is primarily forced by the horizontal temperature gradient between the air over the elevated plateau (representing Mackenzie Basin) and the air at the same elevation over the plains (representing the Canterbury Plains). However, forcings that increase this temperature gradient (such as cold air advection by the seabreeze or higher soil moisture over the plains) can influence the intensity of the CPB by about 2 m s^{-1}.

Time series of the u-component of wind from a grid-point on the plateau (indicated by an arrow in Fig. 2) extracted from the lowest computational level (25 m AGL) are presented in Fig. 11 for all twelve simulations. For the plateau experiment, while the maximum intensity of wind increased by 2 m s^{-1} between the dry and the wet runs (Fig. 11(a)), the difference between the wet runs is negligible. However, there is a significant difference in the onset of the

Fig. 11 **Time series of surface u-component wind at the grid-point on the plateau (marked in Fig. 2) for the (a) plateau, (b) mountain and (c) basin simulations.**

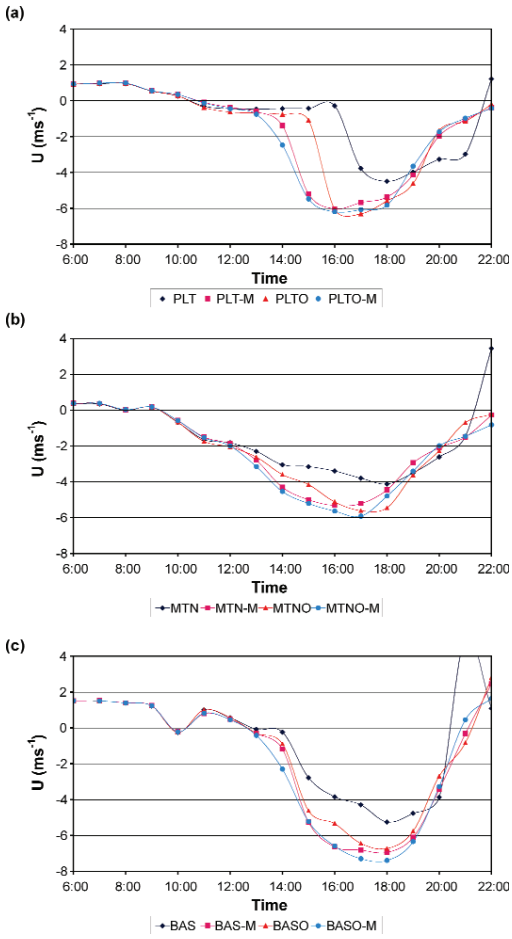

breeze at this location between the runs. When higher soil moisture content over the plains is specified (PLTM experiment), the CPB reaches this location three hours earlier than the dry run. For this topographic configuration, the difference in soil moisture (and hence the boundary-layer development over the plains) seems to have the strongest influence on the intensity of the circulation.

Since the mountain range had already set up an easterly current over the plateau, the intrusion of the CPB into the elevated plateau was not as well defined with the MTN simulations (Fig. 11(b)). There is negligible difference in the maximum intensity of the easterly between these series of runs and the PLT simulations, suggesting that the Alps do not significantly modify forcing of the CPB.

The CPB was detected at about 1400 NZST at the field site for all scenarios for the basin simulations (Fig. 11(c)). The difference from the two other configurations was that the horizontal temperature gradients have to be strong enough across the eastern ridge, so that the density current can overwhelm the upslope flows opposing it from the basin side, before propagating westward. The difference in maximum intensity of the wind between the dry and wet runs is about 2 m s^{-1} (the same as the other two sets of runs), although there is little difference between the BAS-M and BASO-M. This reinforces the conclusion that the ocean has a marginal forcing effect on the CPB.

Conclusions

Twelve two-dimensional numerical simulations, testing three different topographic configurations and soil moisture variation, were performed to confirm that the Canterbury Plains Breeze (CPB) is a regional-scale mesoscale circulation generated by the horizontal temperature gradient between the air over the basin and the air at the same level over the Canterbury Plains. The numerical simulations show that the CPB is greatly modified by the 'basin' topography and the difference in land-surface characteristics between the basin and the plains. Sensitivity runs show that variation of land-surface characteristics, such as land-sea discontinuity and soil moisture gradient, influence the intensity of this density current by up to 2 m s^{-1}. The numerical experiments also show that the sea-breeze and CPB are two different circulation systems generated by different physical forcing.

Acknowledgments

This research was undertaken with a grant from the Marsden Fund (grant number UOC602), awarded by the Royal Society of New Zealand. The leading author performed the numerical runs while he was a visiting fellow at Pacific Northwest Laboratories in Richland, Washington. We would like to thank Drs Sharon Zhong and Jerome Fast for assistance with running RAMS, and Dr Whiteman for providing funding during the stay. We would also like to thank the support staff at the Geography Department of the University of Canterbury for their invaluable assistance.

References

Anthes, R.A. 1978. The height of the planetary boundary layer and the production of circulation in a sea breeze model. *J. Atmos. Sci., 35,* 1231-9.

Atkinson, B.W. 1981. *Meso-scale Atmospheric Circulations*. Academic Press, New York, 495 pp.

Barry, R.G. 1992. *Mountain Weather and Climate.* 2d Ed. Routledge, New York, 402 pp.

Bossert, J.E. and Cotton, W.R. 1994. Regional-scale flows in mountainous terrain. Part II: Simplified numerical experiments. *Mon. Weath. Rev., 122*, 1472-89.

Businger, J.A., Wyngaard, C.J., Izumi, Y. and Bradley, E.F. 1971. Flux-profile relationship in the atmospheric surface layer. *J. Atmos. Sci., 28*, 181-9.

Chen, C. and Cotton, W.R. 1983. A one-dimensional simulation of the stratocumulus-capped mixed layer. *Bound. Lay. Met., 25*, 289-321.

Defant, F. 1951. Local winds. *Compendium of Meteorology,* American Meteorological Society, 655-72.

De Wekker, S.F.J., Zhong, S., Fast, J.D. and Whiteman, C.D. 1998. A numerical study of the thermally driven plain-to-basin wind over idealized basin topographies. *Jnl appl. Met., 37*, 606-22.

Doran, J.C. and Zhong, S. 2000. Thermally driven gap winds into the Mexico City Basin. *Jnl appl. Met., 39*, 1330-40.

Fast, J.D., Zhong, S. and Whiteman, C.D. 1996. Boundary layer evolution within a canyonland basin. Part II: numerical simulations of nocturnal flows and heat budgets. *Jnl appl. Met., 35*, 2162-78.

Flohn, H. 1969. Local wind systems. *World Survey of Climatology, Vol. 2*, Elsevier, New York, 139-71.

Helfand, H.M. and Labraga, J.C. 1988. Design of a nonsingular level 2.5 second-order closure model for the prediction of atmospheric turbulence. *J. Atmos. Sci., 45*, 113-32.

Kimura, F. and Kuwagata, T. 1993. Thermally induced wind passing from plain to basin over a mountain range. *Jnl appl. Met., 32*, 1538-47.

Klemp, J.B. and Wilhelmson, R.B. 1978a. The simulation of three-dimensional convective storm dynamics. *J. Atmos. Sci., 35*, 1070-96.

Klemp, J.B. and Wilhelmson, R.B. 1978b. Simulations of right- to left-moving storms produced through storm splitting. *J. Atmos. Sci., 35,* 1097-110.

Kossmann, M., Sturman, A.P., Zawar-Reza, P., McGowan, H.A., Oliphant, A.J., Owens, I.F. and Spronken-Smith, R.A. 2002. Analysis of the wind field and heat budget in an alpine lake basin during summertime fair weather conditions, *Met. Atmos. Phys., 81*, 27-52.

Kurita, H., Ueda, H. and Mitsumoto, S. 1990. Combination of local wind systems under light gradient wind conditions and its contribution to the long-range transport of air pollutants. *Jnl appl. Met., 29*, 331-48.

Louis, J-.F. 1979. A parameteric model of vertical eddy fluxes in the atmosphere. *Bound. Lay. Met., 17,* 187-202.

Lu, R. and Turco, R.P. 1994. Air pollutant transport in a coastal environment. Part I: Two-dimensional simulations of sea-breeze and mountain effects. *J. Atmos. Sci., 51,* 2285-308.

Mahrer, Y. and Pielke, R.A. 1977. The effects of topography on the sea and land breezes in a two-dimensional numerical model. *Mon. Weath. Rev., 105*, 1151-62.

Mannouji, N. 1982. A numerical experiment on the mountain and valley winds. *J. Met. Soc. Japan, 60,* 1085-105.

McGowan, H.A., Owens, I. and Sturman, A.P. 1995. Thermal and dynamic characteristics of alpine lake breezes, Lake Tekapo, New Zealand. *Bound. Lay. Met., 76*, 3-24.

McGowan, H.A. and Sturman, A.P. 1996. Interacting multi-scale wind systems within an alpine basin, Lake Tekapo, New Zealand. *Met. Atmos. Phys., 58,* 165-77.

Mellor, G.L. and Yamada, T. 1974. A hierarchy of turbulence closure models for planetary boundary layers. *J. Atmos. Sci., 31*, 1791-806.

Mellor, G.L. and Yamada, T. 1982. Development of a turbulence closure model for geophysical fluid problems. *Rev. Geophys. Space Phys., 20,* 851-75.

Monin, A.S. and Obukhov, A.M. 1954. Basic regularity in turbulent mixing in the surface layer of the atmosphere. *Akad. Nauk. S.S.S.R. Trud. Geofiz. Inst., 24,* 163-87.

Oke, T.R. 1992. *Boundary Layer Climates.* 2nd Ed. Routledge, London, 435 pp.

Pielke, R.A., Cotton, W.R. Walko, R.L., Tremback, C.J., Lyons, W.A., Grasso, L.D., Nicholls, M.E., Moran, M.D., Wesley, D.A., Lee, T.J. and Copeland, J.H. 1992. A comprehensive meteorological modelling system – RAMS. *Met. Atmos. Phys., 49*, 69-91.

Pielke, R.A. 2002. *Mesoscale Meteorological Modelling.* 2nd Ed. Academic Press, San Diego, 676 pp.

Smagorinsky, J. 1963. General circulation experiments with the primitive equations. Part I, The basic experiment. *Mon. Weath. Rev., 91,* 99-164.

Sturman, A.P., Bradley, S., Drummond, P., Grant, K., Gudiksen, P., Hipkin, V., Kossmann, M., McGowan, H.A., Oliphant, A., Owens, I.F., Powell, S., Spronken-Smith, R.A., Webb, T. and Zawar-Reza, P. 2003. The Lake Tekapo Experiment (LTEX): an investigation of atmospheric boundary layer processes in complex terrain. *Bull. Am. Met. Soc., 84*, 371-80.

Tripoli, G.J. and Cotton W.R. 1981. The use of ice-liquid water potential temperature as a variable in deep atmospheric models. *Mon. Weath. Rev., 109,* 1094-102.

Whiteman, C.D. 2000. *Mountain Meteorology: fundamentals and applications.* Oxford University Press, New York, 355 pp.

Whiteman, C.D., Zhong, S., Bian, X., Fast, J.D. and Doran J.C. 2000. Boundary layer evolution and regional-scale diurnal circulations over the Mexico Basin and Mexican Plateau. *J. Geophys. Res., 105*, 10081-102.

Zawar-Reza, P. 2000. Numerical modelling of thermally induced regional and local scale Flows in Mackenzie Basin, New Zealand. Unpublished Ph.D. thesis, University of Canterbury.

Zawar-Reza, P., McGowan, H.A., Sturman A.P. and Kossmann, M. 2004. Numerical simulations of wind and temperature structure within an Alpine lake basin. *Met. Atmos. Phys., 86*, 245-60.

Zhong, S., Fast, J.D. and Bian, X. 1996. A case study of the Great Plains low-level jet using profiler network data and a high-resolution mesoscale model. *Mon. Weath. Rev., 124*, 785-806.